ACS APPLIED MATERIALS & INTERFACES

Research Article

www.acsami.org

# Facile Preparation of Biocompatible and Robust Fluorescent Polymeric Nanoparticles via PEGylation and Cross-Linking

Haiyin Li,*[,†] Xiqi Zhang,*[,‡,§] Xiaoyong Zhang,[‡] Ke Wang,[‡] Hongliang Liu,[§] and Yen Wei*[,‡]

[†]College of Chemistry and Pharmaceutical Sciences, Qingdao Agriculture University, Qingdao, 266109, P. R. China

[‡]Department of Chemistry and the Tsinghua Center for Frontier Polymer Research, Tsinghua University, Beijing, 100084, P. R. China

[§]Laboratory of Bio-Inspired Smart Interface Science, Technical Institute of Physics and Chemistry, Chinese Academy of Sciences, Beijing, 100190, P. R. China

Supporting Information

**ABSTRACT:** Novel cross-linked copolymers of **PEG-IM-PhNH$_2$** are successfully synthesized through PEGylation via radical polymerization of 2-isocyanatoethyl methacrylate and poly(ethylene glycol) monomethyl ether methacylate and subsequent cross-linking with an amino-terminated aggregation-induced emission fluorogen. Such obtained amphiphilic copolymers can self-assemble to form uniform fluorescent polymeric nanoparticles (FPNs) and be utilized for cell imaging. These cross-linked FPNs are demonstrated good water dispersibility with ultralow critical micelle concentration (~0.002 mg mL$^{-1}$), uniform morphology (98 ± 2 nm), high red fluorescence quantum yield, and excellent biocompatibility. More importantly, this novel strategy of fabricating cross-linked FPNs paves the way to the future development of more robust and biocompatible fluorescent bioprobes.

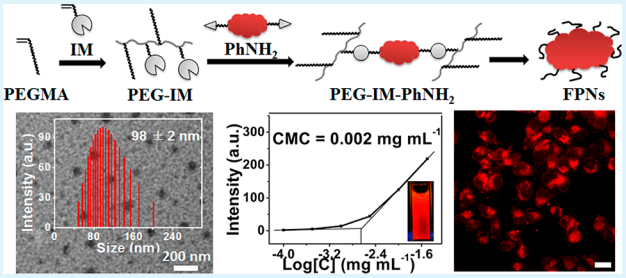


**KEYWORDS:** *PEGylation, cross-linking, aggregation-induced emission, fluorescent polymeric nanoparticles, critical micelle concentration, cell imaging*

## 1. INTRODUCTION

Fluorescent polymeric nanoparticles (FPNs) have attracted great research attention owing to their large Stokes shifts, excellent photostability, and large absorption cross sections, and become widely used probes for bioimaging and biomedical applications.[1−6] So far, many polymerizable dyes such as rhodamines,[7] fluoresceins,[8] 1,8-naphthalimides,[9] and coumarins,[10] have been utilized for fabricating FPNs based on side-chain functionalized polymers. In addition, fluorescent conjugated polymers, or main-chain functionalized polymers, have been extensively investigated for various in vitro and in vivo bioimaging applications.[11−13] However, many conventional dyes in FPNs are planar conjugated structures, which are easy to quench fluorescence in aggregated state because of strong intermolecular $\pi-\pi$ interactions. This phenomenon is also called aggregation-causing quenching effect.[14−16] Generally, most light-emitting materials for real biomedical application are at aggregated state, it seems impossible to avoid this annoying fluorescent quenching. To overcome this limitation, aggregation-induced emission (AIE) fluorogens, which emit intensely in aggregated state without quenching effect, have emerged and already been utilized to construct fluorescent chemosensors and bioprobes.[17−23]

Recently, some strategies like noncovalent and covalent methods of fabricating FPNs based on AIE fluorogens have been reported, and the covalent one is demonstrated with more stability than the noncovalent one in the aspect of preventing dye leakage.[24,25] Owing to great advances in fabrication technology, FPNs based on AIE dyes with intense fluorescence, high dispersibility and excellent biocompatibility have been prepared for cell imaging applications.[26−28] However, more versatile and robust fabricating strategies are extremely desired, like stable dispersion in aqueous solution, as the nanoparticles from self-assembly are often unstable when their concentrations are below critical micelle concentrations (CMC).[29] To this end, fabricating FPNs via cross-linking strategy has been reported to construct AIE-based amphiphilic copolymers with low CMC.[30,31] In our previous study, an AIE chain transfer agent has been utilized to prepare biocompatible cross-linked FPNs through reversible addition−fragmentation transfer polymerization. Such FPNs showed intense blue emssion and high stability in physiological solution with low CMC values (0.155 and 0.178 mg mL$^{-1}$).[30] Another kind of AIE-based cross-linked FPNs (**EP-CL**) has also been prepared in our group by means of emulsion polymerization and anhydride cross-linking. These **EP-CL** FPNs were endowed with even lower CMC (~0.020

Received: December 3, 2014
Accepted: February 6, 2015
Published: February 6, 2015




DOI: 10.1021/am5085308
ACS Appl. Mater. Interfaces 2015, 7, 4241−4246

mg $mL^{-1}$), which broaden their application scopes for cell imaging.[31] Polyethylene glycol (PEG) is an amphiphilic polymer comprised of repeating ethylene oxide subunits, which is approved by FDA previously for applications in various biomedical areas, and widely utilized to improve water dispersibility and biocompatibility in the area of surface modifications.[32] Therefore, it is of great scientific interest to develop novel synthetic routes for the preparation of biocompatible and robust cross-linked FPNs, especially through PEGylation and cross-linking.

In this work, novel cross-linked copolymers, **PEG-IM-PhNH$_2$**, are successfully synthesized through PEGylation via radical polymerization of 2-isocyanatoethyl methacrylate (IM) and poly(ethylene glycol) monomethyl ether methacylate (PEGMA) to afford an isocyanate-containing macromolecular intermediate (**PEG-IM**), and subsequent cross-linking of **PEG-IM** with an amino-terminated AIE-based fluorogen (**PhNH$_2$**). Such obtained amphiphilic copolymers tend to self-assemble to form uniform nanoparticles (Scheme 1). To prove the successful synthesis of **PEG-IM-PhNH$_2$** and characterize the performances of the as-prepared FPNs, some experiments including gel permeation chromatography (GPC), $^1$H NMR spectroscopy, Fourier transform infrared spectroscopy (FT-IR) spectroscopy, X-ray photoelectron spectroscopy (XPS), elemental analysis (EA), transmission electron microscopy (TEM), dynamic light scattering (DLS), UV−visible absorption spectrum (UV), and fluorescence spectra are carried out. Finally, potential biomedical applications of **PEG-IM-PhNH$_2$** FPNs are further evaluated by investigating their biocompatibilities and cell uptake behaviors.

**Scheme 1. Fabricating Route of PEG-IM-PhNH$_2$ Copolymers through PEGylation via Radical Polymerization of PEGMA and IM to Afford PEG-IM, and Subsequent Crosslinking with an AIE-Based Fluorogen (PhNH$_2$), and Subsequent Self-Assembly of the Copolymers to Afford FPNs**

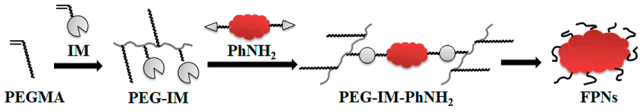


## 2. EXPERIMENTAL SECTION

**2.1. Materials and Measurements.** *N*,*N*-dimethylformamide (DMF), 1-bromooctadecane, phenothiazine, 1,2-dichloroethane, 4-aminobenzyl cyanide, tetrabutylammonium hydroxide (0.8 M in methanol), phosphoryl chloride, and 2-isocyanatoethyl methacrylate (IM) were purchased from Alfa Aesar. PEGMA ($M_n$ = 950 Da) was bought from Aldrich company. All other materials were purchased from commercial sources. Ultrapure water obtained from Milli-Q was used in the experiments.

The characterization of the as-prepared copolymers by GPC (Shimadzu LC-20AD pump system), $^1$H NMR spectra (Mercury-Plus 300 MHz spectrometer), FT-IR spectra (Shimadzu Spectrum 8400 spectrometer), and XPS (VGESCALAB 220-IXL spectrometer) were the same as our previous reference.[31] The size distribution and morphology of the **PEG-IM-PhNH$_2$** FPNs were determined with Zeta Plus apparatus (ZetaPlus, Brookhaven Instruments, Holtsville, NY), HT7700 microscope (Hitachi, Japan) according our previous reference.[30] UV (UV/vis/NIR 2600 spectrometer) and Fluorescence spectra (F-4600 spectrometer) were used to determine the optical properties of the **PEG-IM-PhNH$_2$** FPNs with the same detail conditions reported in our previous literature.[30]

**2.2. Preparation of PEG-IM-PhNH$_2$.** The AIE monomer, **PhNH$_2$**, was prepared according to our previous literature.[27] For the synthesis of **PEG-IM-PhNH$_2$** copolymers, a PEG monomer (PEGMA) and an isocyanate monomer (IM) were copolymerized first using a radical initiator (AIBN) dissolved in ethyl acetate, and through radical polymerization to afford a macromolecular isocyanate intermediate (**PEG-IM**), and then subsequent cross-linking of **PEG-IM** with **PhNH$_2$** via facile combination of isocyanate and amino groups was carried out to obtain the resulting cross-linked copolymers, **PEG-IM-PhNH$_2$** (Scheme 2). In detail, IM (31 mg, 0.20 mmol), PEGMA (190 mg, 0.20 mmol), and AIBN (5.0 mg) were dispersed in 6 mL of ethyl acetate. The above mixture was introduced into Schlenk tube, and purged with nitrogen for a period of 30 min, and then put into an oil bath, as the reaction temperature at 80 °C for 12 h. Followed by the addition of **PhNH$_2$** (37 mg, 0.05 mmol), which was previously dissolved in ethyl acetate (4 mL), and the reaction took place at room temperature for 0.5 h. Then, stopped the reaction and dialyzed using dialysis membranes ($M_w$ ≈ 7000 Da, cutoff) against tap water and ethanol for 24 and 6 h, respectively. Finally, the dispersion of **PEG-IM-PhNH$_2$** in dialysis bag was purified by freeze-drying.

**Scheme 2. Synthetic Route of PEG-IM-PhNH$_2$[a]**

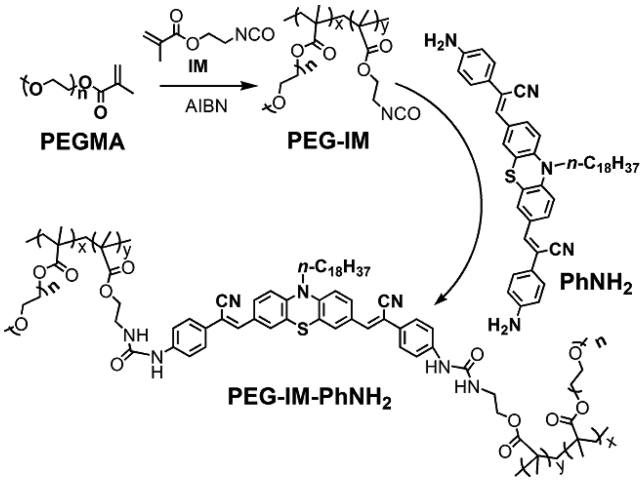


[a]PEGylation through radical polymerization of PEGMA and IM to obtain **PEG-IM** and subsequent facile crosslinking with **PhNH$_2$** to obtain the cross-linked copolymer, **PEG-IM-PhNH$_2$**.

**2.3. Cytotoxicity of PEG-IM-PhNH$_2$ FPNs.** Different concentrations of **PEG-IM-PhNH$_2$** FPNs were employed in the incubation of A549 cells, and the cell morphology was examined to determine the cytotoxicity of **PEG-IM-PhNH$_2$** FPNs. A Leica optical microscopy (Germany) was used to observe the morphology of cells, while the detail of experimental conditions was consistent with our previous report.[30]

Cell counting kit-8 (CCK-8) assay was carried out to evaluate the cell viability of **PEG-IM-PhNH$_2$** FPNs on A549 cells. The cells were incubated with different concentrations of **PEG-IM-PhNH$_2$** FPNs (10, 20, 40, 80, and 120 $\mu$g $mL^{-1}$). The percent reduction of CCK-8 dye was compared to control cells (no exposure to **PEG-IM-PhNH$_2$** FPNs), which represented 100% CCK-8 reduction. The detail of experimental conditions was the same as our previous reference.[30]

**2.4. Confocal Microscopic Imaging of Cells Incubated with PEG-IM-PhNH$_2$ FPNs.** A confocal laser scanning microscope (Zeiss 710 3-channel, Germany) was used to record the confocal microscopic imaging of A549 cells incubated with **PEG-IM-PhNH$_2$** FPNs. The excitation wavelength for A549 cells was set as 488 nm. The cell culture conditions have already been reported in our previous reference.[30]


DOI: 10.1021/am5085308
ACS Appl. Mater. Interfaces 2015, 7, 4241−4246

## 3. RESULTS AND DISCUSSIONS

**3.1. Characterization of PEG-IM-PhNH$_2$ FPNs.** In the synthesis of **PEG-IM-PhNH$_2$** copolymers, PEGylation was first carried out by radical polymerization between IM and PEGMA using a radical initiator of AIBN in ethyl acetate to obtain **PEG-IM**, then subsequent cross-linking of **PEG-IM** with **PhNH$_2$** was conducted to obtain the cross-linked copolymers, **PEG-IM-PhNH$_2$** (Scheme 2). The feed molar ratio of PEGMA, IM, and **PhNH$_2$** was designed as 4:4:1, respectively. The number-average molecular weight value of **PEG-IM-PhNH$_2$** was determined by GPC, which indicated that the value was 167800 Da with a polydispersity index of 1.44. To confirm the successful synthesis of **PEG-IM-PhNH$_2$** copolymers, $^1$H NMR spectra of the reactants and resulting copolymer were conducted for comparison (Figure 1A). After PEGylation and

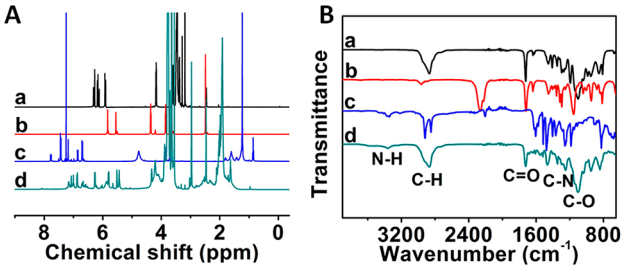


**Figure 1.** (A) $^1$H NMR spectra of PEGMA (a), IM (b), **PhNH$_2$** (c), and **PEG-IM-PhNH$_2$** (d), the characteristic chemical shifts of the methylene group of PEGMA located at 4.2 and 3.5 ppm, and the methylene group of IM located at 4.4 and 3.9 ppm are found in **PEG-IM-PhNH$_2$**, meanwhile, the amino group of **PhNH$_2$** located at 4.8 ppm is disappeared and new N−H group at 6.3 ppm is observed in the **PEG-IM-PhNH$_2$**, demonstrating the successful synthesis of **PEG-IM-PhNH$_2$**; (B) FT-IR spectra of PEGMA (a), IM (b), **PhNH$_2$** (c), and **PEG-IM-PhNH$_2$** (d), obvious stretching vibration peaks of N−H (3360 cm$^{-1}$), C−H (2870 cm$^{-1}$), C═O (1725 cm$^{-1}$), C−N (1249 cm$^{-1}$), and C−O (1100 cm$^{-1}$) are observed in **PEG-IM-PhNH$_2$**, indicating their successful preparation.

consecutive cross-linking with **PhNH$_2$**, the characteristic chemical shifts of the methylene group of PEGMA located at 4.2 and 3.5 ppm, and the methylene group of IM located at 4.4 and 3.9 ppm were found in **PEG-IM-PhNH$_2$**. Meanwhile, the amino group of **PhNH$_2$** located at 4.8 ppm was disappeared and new N−H group at 6.3 ppm was observed in the **PEG-IM-PhNH$_2$**, demonstrating the successful synthesis of **PEG-IM-PhNH$_2$**. From the $^1$H NMR spectrum of **PEG-IM-PhNH$_2$**, the ratio of PEGMA and IM units ($x/y$) was calculated as 2/1 in the final composition of the polymers. As the degree of polymerization is unknown, the conversion of the polymerization is unavailable.

Furthermore, successful synthesis of **PEG-IM-PhNH$_2$** was also proven by FT-IR (Figure 1B). Two characteristic peaks, which represented for the stretching vibration of $CH_2$ group, were observed in **PhNH$_2$** located at 2919 and 2847 cm$^{-1}$. Meanwhile, several peaks distributed at the range of 1450−1600 cm$^{-1}$ were found, which were ascribed to the stretching vibration of aromatic rings. After PEGylation and subsequent cross-linking with **PhNH$_2$**, obvious stretching vibration peaks of N−H (3360 cm$^{-1}$), C−H (2870 cm$^{-1}$), C═O (1725 cm$^{-1}$), C−N (1249 cm$^{-1}$), and C−O (1100 cm$^{-1}$) were all observed in **PEG-IM-PhNH$_2$**, which demonstrated the successful formation of this copolymers.

XPS was also carried out to determine the chemical composition of the prepared **PEG-IM-PhNH$_2$**. As shown in Figure 2 and Supporting Information Figure S1, the XPS result

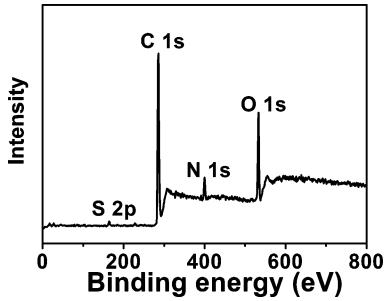


**Figure 2.** XPS spectrum of **PEG-IM-PhNH$_2$** FPNs indicating the presence of carbon, nitrogen, oxygen, and sulfur.

indicated that carbon was the major component, while nitrogen, oxygen, and sulfur were the other minor components. It could be found two peaks in the C 1s XPS spectrum of **PEG-IM-PhNH$_2$**. The main peak was at ∼285 eV, while the shoulder peak was at ∼286 eV, which were attributed to sp$^2$ and sp$^3$ carbon atoms, respectively. The N 1s, O 1s, and S 2p spectra of **PEG-IM-PhNH$_2$** showed peak centered at ∼399, ∼ 532, and ∼164 eV, respectively. The ratio of **PhNH$_2$** in the resulting **PEG-IM-PhNH$_2$** has significant effect on their fluorescence quantum yields and cytotoxicity. Therefore, elemental analysis (EA) of **PEG-IM-PhNH$_2$** was detected with an Elementar Vario EL Elemental Analyzer (Germany). The overall wt % of elements existing in **PEG-IM-PhNH$_2$** was ∼55.48:8.95:1.49 for C/H/N, respectively. The content of **PhNH$_2$** in the resulting copolymer was calculated from the EA result and given as 11% for the mass fraction. Moreover, we have synthesized other two new copolymers by adjusting the content of **PhNH$_2$**, they are **PEG-IM-0.5PhNH$_2$** and **PEG-IM-0.25PhNH$_2$** with 50% and 25% of **PhNH$_2$** as comparing with that in **PEG-IM-PhNH$_2$**, respectively. The fluorescence quantum yield and cytotoxicity of these three copolymers would be discussed later.

Self-assembly of amphiphilic block copolymers into nanoparticles has been widely studied ranging from biomedical to nanometer-scale enzymatic reactors.[33,34] Therefore, the size distribution of **PEG-IM-PhNH$_2$** FPNs has been determined in PBS to confirm the particles sizes. The results showed that the size distribution of **PEG-IM-PhNH$_2$** FPNs was 98 ± 2 nm, with a polydispersity index of 0.209 (Figure 3A). Meanwhile, the morphology of the resulting **PEG-IM-PhNH$_2$** FPNs was further confirmed by the TEM study (Figure 3B). Some spherical nanoparticles could be clearly observed with diameters at the range of 40−70 nm, demonstrating the as-

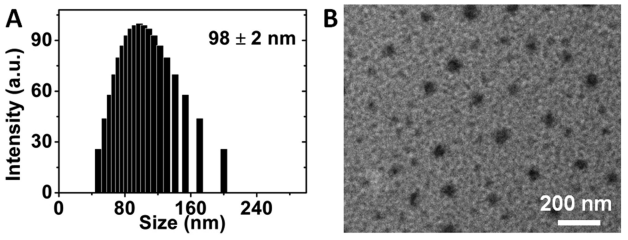


**Figure 3.** (A) DLS result of **PEG-IM-PhNH$_2$** FPNs in PBS; (B) TEM image of **PEG-IM-PhNH$_2$** FPNs dispersed in water, scale bar = 200 nm.


DOI: 10.1021/am5085308
ACS Appl. Mater. Interfaces 2015, 7, 4241−4246

prepared copolymers could self-assemble to form FPNs. It could be noted that the size of nanoparticles observed by TEM were smaller than that by DLS, which might be owing to the shrinkage of FPNs at dry phase.

The amphiphilic feature of the as-prepared copolymers endowed them the tendency to self-assemble into nanoparticles when **PEG-IM-PhNH$_2$** were dispersed in water. Here, the hydrophobic AIE components tended to aggregate into the cores, while the surfaces were covered the hydrophilic PEG segments. Therefore, the FPNs are expected to have high water dispersibility and bright fluorescent emission. Hence, the UV absorption spectrum of **PEG-IM-PhNH$_2$** FPNs in water was detected (Figure 4A). It could be found that three continuous

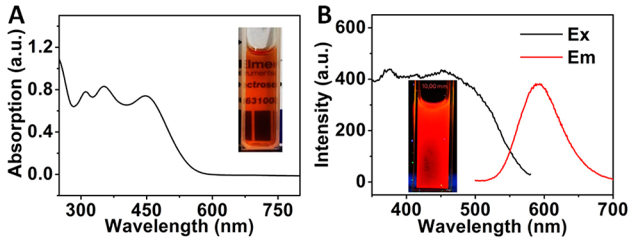


**Figure 4.** (A) UV−vis spectrum of **PEG-IM-PhNH$_2$** FPNs, the inset is the visible image of **PEG-IM-PhNH$_2$** FPNs in water; (B) Fluorescence excitation (Ex) and emission (Em) spectra of **PEG-IM-PhNH$_2$** FPNs, the inset is the fluorescent image of **PEG-IM-PhNH$_2$** FPNs under UV light (excited at 365 nm).

absorption peaks were located at 310, 352, and 448 nm, representing for the different conjugated systems from the parts to the whole. In the previous report, when the FPNs were formed in the UV solutions, the entire spectrum started to increase from 800 nm owing to the Mie effect, which was considered as the dispersion of nanoparticles in the solution.[27] However, it is interestingly in this work to find that no increase of the absorption in the UV spectrum from 800 to 600 nm, which might be caused by the high dispersibility of the FPNs in water after the introduction of PEG components. The inset of Figure 4A directly proved these FPNs had high water dispersibility with high transparency.

Because of the aggregation effect of AIE fluorogens inside the FPNs, bright red fluorescence was clearly observed when **PEG-IM-PhNH$_2$** FPNs was dispersed in water (inset of Figure 4B). To quantitatively determine their optical performances in water, the PL spectra of **PEG-IM-PhNH$_2$** FPNs were recorded. The results showed that the maximum emission wavelength was 593 nm. Meanwhile, the fluorescence excitation wavelength could be divided into three peaks (375, 415, and 450 nm), which was consistent with the absorption result. Fluorescence emission spectra of **PEG-IM-PhNH$_2$**, **PEG-IM-0.5PhNH$_2$**, and **PEG-IM-0.25PhNH$_2$** FPNs were showed in Supporting Information Figure S2. The results proved blue-shift of the emission when the content of **PhNH$_2$** in the copolymers decreased. The fluorescent quantum yield of the **PEG-IM-PhNH$_2$** FPNs was determined as ∼14% using Rhodamine 6G in ethanol as the reference dye. The fluorescence quantum yields of **PEG-IM-0.5PhNH$_2$** and **PEG-IM-0.25PhNH$_2$** were calculated as ∼12% and ∼9%, respectively. For comparison, the fluorescent quantum yield of **PhNH$_2$** determined in THF was 7.0%.

Photostability is one of the most important factors for the development of fluorescent bioprobes. The fluorescent bioprobe should be photostable under continual irradiation for long-term tracking and treatment.[35] Thus, the photostability of **PEG-IM-PhNH$_2$** FPNs in water was determined (Figure 5A).

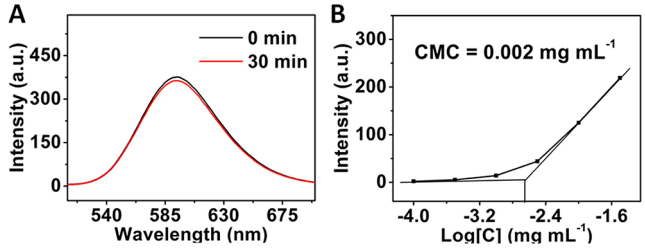


**Figure 5.** (A) PL spectra of **PEG-IM-PhNH$_2$** FPNs before and after irradiated with UV lamp of 365 nm for a period of 30 min; (B) Intensity of the fluorescence emission vs the logarithm of the concentration of **PEG-IM-PhNH$_2$** ($\lambda_{ex}$ = 488 nm, $\lambda_{em}$ = 593 nm).

The result showed no obvious fluorescent bleaching were detected after irradiated by a UV lamp of 365 nm for a period of 30 min, demonstrating remarkable photostability and high resistance to photobleaching of these **PEG-IM-PhNH$_2$** FPNs. It is very annoying that the CMC problem often hinders the application of FPNs at low concentration. To overcome the issue of CMC, novel cross-linking strategy by facile combining the isocyanate and amino groups has been adopted in this work. Thanks to the superiority of AIE-based fluorogens, the as-prepared copolymers emitted little fluorescence when they are dispersed in the aqueous solution below CMC. However, when the concentration is higher than CMC, the fluorescent emission of these copolymers increases rapidly due to the aggregation of the AIE-based fluorogens.[36] Then, we tracked the change of the maximum fluorescent emission intensity under different aggregated state of **PEG-IM-PhNH$_2$** in water to obtain the CMC value. In this case, the intensity of fluorescence emission vs the logarithm of different concentration of **PEG-IM-PhNH$_2$** was determined to track the CMC value by the tangent method. The results showed that ultralow CMC value of 0.002 mg mL$^{-1}$ was obtained in **PEG-IM-PhNH$_2$** FPNs (Figure 5B), which made it become the lowest CMC in the reported cross-linked FPNs. Such ultralow CMC of **PEG-IM-PhNH$_2$** FPNs might be due to the introduction of PEG segments, which greatly increased the dispersibility of the FPNs, and would be highly beneficial to broaden the concentration range of the FPNs for biomedical applications.

**3.2. Biocompatibility.** The cell viability of **PEG-IM-PhNH$_2$** FPNs was evaluated to test their biocompatibilities. A549 cells were incubated with different concentrations of **PEG-IM-PhNH$_2$** FPNs for 24 h, and observed by optical microscopy to examine the influence of the FPNs to these cells (Figure 6A-C). The result showed high cell viability when the cells were incubated with either 10 or 80 $\mu$g mL$^{-1}$ of **PEG-IM-PhNH$_2$** FPNs, which demonstrated the FPNs were highly biocompatible. Furthermore, to quantitatively characterize the cytocompatibility of these nanoparticles, CCK-8 assay was used to determine their cell viabilities to A549 cells. It could be found in Figure 6D that cell viability did not decrease, when the cells were incubated with different concentrations of **PEG-IM-PhNH$_2$** FPNs (10−120 $\mu$g mL$^{-1}$) either for 8 or 24 h. Even at high concentration of 120 $\mu$g mL$^{-1}$ for a period of 24 h, high cell viability value was still achieved at 95%, indicating highly potential of these FPNs for cell imaging. Cell viability of **PEG-IM-0.5PhNH$_2$** and **PEG-IM-0.25PhNH$_2$** FPNs for 8 and 24 h


DOI: 10.1021/am5085308
ACS Appl. Mater. Interfaces 2015, 7, 4241−4246

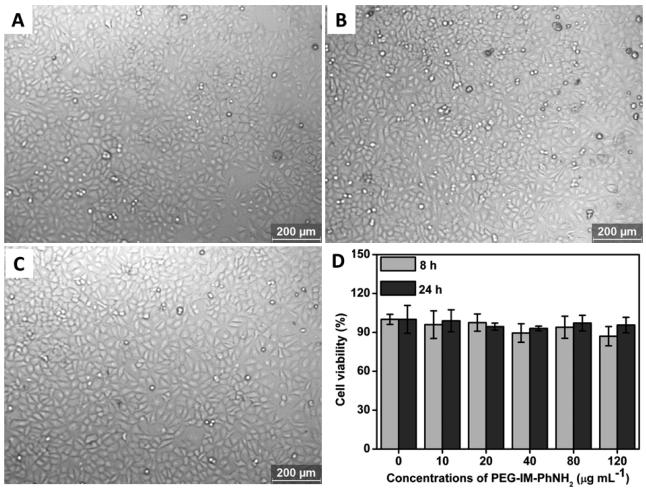


**Figure 6.** (A–C) optical microscopy images of A549 cells when incubated with different concentrations of **PEG-IM-PhNH$_2$** FPNs for 24 h: (A) control cells, (B) 10 $\mu$g mL$^{-1}$, (C) 80 $\mu$g mL$^{-1}$; (D) cell viability of A549 cells when incubated with different concentrations of **PEG-IM-PhNH$_2$** FPNs for 8 and 24 h. Cell viability was determined by the CCK-8 assay.

were also determined, and shown in Supporting Information Figure S3. The results demonstrated that these two FPNs had high cell viability as that of **PEG-IM-PhNH$_2$** FPNs.

**3.3. Cell Imaging.** Confocal Laser Scanning Microscope (CLSM) was conducted to further evaluate the cell uptake style of **PEG-IM-PhNH$_2$** FPNs and explore their cell imaging applications. As shown in Figure 7, after the cell was incubated

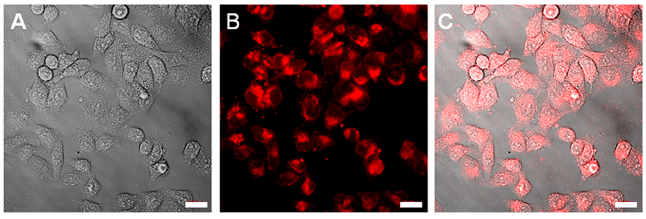


**Figure 7.** CLSM images of A549 cells when incubated with 10 $\mu$g mL$^{-1}$ of **PEG-IM-PhNH$_2$** FPNs for 3 h. (A) bright field, (B) excited with 488 nm laser, (C) merged image of A and B. Scale bar = 20 $\mu$m.

with 10 $\mu$g mL$^{-1}$ of **PEG-IM-PhNH$_2$** FPNs, bright red fluorescence could be detected at the cell region. Moreover, many dim areas inside the cells were found, which indicated the possible position of the cell nucleus (Figure 7B). As compared to the nucleus pore of the cells, **PEG-IM-PhNH$_2$** FPNs could facilely stain the cells at cytoplasm without entrancing into the cell nucleus. Due to the intense emission derived from the aggregation of **PhNH$_2$**, strong red fluorescent signal can be detected inside the cells, which is greatly beneficial to cell imaging.

In the previous report, some AIE based cross-linked FPNs have been facilely prepared through radical polymerization, which demonstrated uniform morphology and intense fluorescence for cell imaging.[30,31] However, those FPNs are limited for biomedical application due to the instability in the highly dilute solution or the lack of biocompatible elements (e.g., PEG) for satisfactory metabolic behavior. As compared to the previous references, **PEG-IM-PhNH$_2$** FPNs reported in this work have obvious superiority. First, **PEG-IM-PhNH$_2$** FPNs are endowed with ultralow CMC, which can distinctly broaden the scope of application in highly dilute solution. Second, PEG segments are utilized in the construction of FPNs as the major components to meet their biomedical application due to their biocompatible property. Moreover, this novel strategy of PEGylation and cross-linking will provide the opportunity to develop more and more biocompatible and robust fluorescent polymers for biomedical applications.

## 4. CONCLUSIONS

In summary, we have successfully prepared novel cross-linked copolymers (**PEG-IM-PhNH$_2$**) through PEGylation and cross-linking with an amino-terminated AIE-active fluorogen. Such obtained amphiphilic copolymers can self-assemble to form uniform FPNs, which are demonstrated good water dispersibility with ultralow CMC (~0.002 mg mL$^{-1}$), uniform morphology (98 ± 2 nm), high red fluorescence quantum yield, and excellent biocompatibility for cell imaging. More importantly, this novel strategy of fabricating cross-linked FPNs paves the way to the future development of more biocompatible and robust fluorescent bioprobes.

## ■ ASSOCIATED CONTENT

### Ⓢ Supporting Information

XPS spectra of **PEG-IM-PhNH$_2$** FPNs, fluorescence emission spectra of **PEG-IM-PhNH$_2$**, **PEG-IM-0.5PhNH$_2$**, and **PEG-IM-0.25PhNH$_2$** FPNs, and cell viabilities of **PEG-IM-0.5PhNH$_2$** and **PEG-IM-0.25PhNH$_2$** FPNs. This material is available free of charge via the Internet at http://pubs.acs.org.

## ■ AUTHOR INFORMATION

### Corresponding Authors

*E-mail: lhaiyin894@126.com.
*E-mail: xqzhang@mail.ipc.ac.cn.
*E-mail: weiyen@tsinghua.edu.cn.

### Notes

The authors declare no competing financial interest.

## ■ ACKNOWLEDGMENTS

This research was supported by the National Science Foundation of China (Nos. 21134004, 21201108, 51363016), and the National 973 Project (No. 2011CB935700), China Postdoctoral Science Foundation (2012M520243, 2013T60100), the basic research program of Qingdao (14-2-4-102-jch), High-level Science Foundation of Qingdao Agriculture University (631334).

## ■ REFERENCES

(1) Breul, A. M.; Hager, M. D.; Schubert, U. S. Fluorescent Monomers As Building Blocks for Dye Labeled Polymers: Synthesis and Application in Energy Conversion, Biolabeling and Sensors. *Chem. Soc. Rev.* **2013**, *42*, 5366–5407.

(2) Canfarotta, F.; Whitcombe, M. J.; Piletsky, S. A. Polymeric Nanoparticles for Optical Sensing. *Biotechnol. Adv.* **2013**, *31*, 1585–1599.

(3) He, B.; Chu, Y.; Yin, M.; Müllen, K.; An, C.; Shen, J. Fluorescent Nanoparticle Delivered dsRNA Toward Genetic Control of Insect Pests. *Adv. Mater.* **2013**, *25*, 4580–4584.

(4) You, C.-C.; Miranda, O. R.; Gider, B.; Ghosh, P. S.; Kim, I.-B.; Erdogan, B.; Krovi, S. A.; Bunz, U. H. F.; Rotello, V. M. Detection and Identification of Proteins Using Nanoparticle-Fluorescent Polymer "Chemical Nose" Sensors. *Nat. Nanotechnol.* **2007**, *2*, 318–323.



DOI: 10.1021/am5085308
*ACS Appl. Mater. Interfaces* 2015, 7, 4241–4246

(5) Kumar, V.; Adamson, D. H.; Prud'homme, R. K. Fluorescent Polymeric Nanoparticles: Aggregation and Phase Behavior of Pyrene and Amphotericin B Molecules in Nanoparticle Cores. *Small* **2010**, *6*, 2907−2914.
(6) Wang, K.; Yuan, X.; Guo, Z.; Xu, J.; Chen, Y. Red Emissive Cross-Linked Chitosan and Their Nanoparticles for Imaging the Nucleoli of Living Cells. *Carbohydr. Polym.* **2014**, *102*, 699−707.
(7) De Jong, L.; Moreau, X.; Thiéry, A.; Godeau, G.; Grinstaff, M. W.; Barthélémy, P. Amphiphilic Copolymer for Delivery of Xenobiotics: In Vivo Studies in a Freshwater Invertebrate, A Mesostominae Flatworm. *Bioconjugate Chem.* **2008**, *19*, 891−898.
(8) Wu, X.; Price, G. J.; Guy, R. H. Disposition of Nanoparticles and an Associated Lipophilic Permeant following Topical Application to the Skin. *Mol. Pharmaceutics* **2009**, *6*, 1441−1448.
(9) Weizhong, J.; Lingxiang, W.; Yuanlin, S.; Jinjun, J.; Xiaodan, Z.; Dawei, Y.; Chunxue, B. Continuous Intra-Arterial Blood pH Monitoring by a Fiber-Optic Fluorosensor. *IEEE Trans. Biomed. Eng.* **2011**, *58*, 1232−1238.
(10) Zubris, K. A. V.; Khullar, O. V.; Griset, A. P.; Gibbs-Strauss, S.; Frangioni, J. V.; Colson, Y. L.; Grinstaff, M. W. Ease of Synthesis, Controllable Sizes, and In Vivo Large-Animal-Lymph Migration of Polymeric Nanoparticles. *ChemMedChem.* **2010**, *5*, 1435−1438.
(11) Feng, L.; Zhu, C.; Yuan, H.; Liu, L.; Lv, F.; Wang, S. Conjugated Polymer Nanoparticles: Preparation, Properties, Functionalization and Biological Applications. *Chem. Soc. Rev.* **2013**, *42*, 6620−6633.
(12) Feng, X.; Liu, L.; Wang, S.; Zhu, D. Water-Soluble Fluorescent Conjugated Polymers and Their Interactions with Biomacromolecules for Sensitive Biosensors. *Chem. Soc. Rev.* **2010**, *39*, 2411−2419.
(13) Wu, W.; Ye, S.; Yu, G.; Liu, Y.; Qin, J.; Li, Z. Novel Functional Conjugative Hyperbranched Polymers with Aggregation-Induced Emission: Synthesis Through One-Pot "$A_2 + B_4$" Polymerization and Application As Explosive Chemsensors and Pleds. *Macromol. Rapid Commun.* **2012**, *33*, 164−171.
(14) Yuan, W. Z.; Lu, P.; Chen, S.; Lam, J. W.; Wang, Z.; Liu, Y.; Kwok, H. S.; Ma, Y.; Tang, B. Z. Changing the Behavior of Chromophores from Aggregation-Caused Quenching to Aggregation-Induced Emission: Development of Highly Efficient Light Emitters in the Solid State. *Adv. Mater.* **2010**, *22*, 2159−2163.
(15) Chen, M.; Yin, M. Design and Development of Fluorescent Nanostructures for Bioimaging. *Prog. Polym. Sci.* **2014**, *39*, 365−395.
(16) Li, K.; Liu, B. Polymer-Encapsulated Organic Nanoparticles for Fluorescence and Photoacoustic Imaging. *Chem. Soc. Rev.* **2014**, *43*, 6570−6597.
(17) Hong, Y.; Lam, J. W.; Tang, B. Z. Aggregation-Induced Emission. *Chem. Soc. Rev.* **2011**, *40*, 5361−5388.
(18) Zhang, X.; Chi, Z.; Li, H.; Xu, B.; Li, X.; Zhou, W.; Liu, S.; Zhang, Y.; Xu, J. Piezofluorochromism of an Aggregation-Induced Emission Compound Derived from Tetraphenylethylene. *Chem.—Asian J.* **2011**, *6*, 808−811.
(19) Huang, J.; Sun, N.; Dong, Y.; Tang, R.; Lu, P.; Cai, P.; Li, Q.; Ma, D.; Qin, J.; Li, Z. Similar or Totally Different: The Control of Conjugation Degree through Minor Structural Modifications, and Deep-Blue Aggregation-Induced Emission Luminogens for Non-Doped OLEDs. *Adv. Funct. Mater.* **2013**, *23*, 2329−2337.
(20) Zhang, X.; Chi, Z.; Zhang, J.; Li, H.; Xu, B.; Li, X.; Liu, S.; Zhang, Y.; Xu, J. Piezofluorochromic Properties and Mechanism of an Aggregation-Induced Emission Enhancement Compound Containing *N*-Hexyl-Phenothiazine and Anthracene Moieties. *J. Phys. Chem. B* **2011**, *115*, 7606−7611.
(21) Li, D.; Miao, C.; Wang, X.; Yu, X.; Yu, J.; Xu, R. AIE Cation Functionalized Layered Zirconium Phosphate Nanoplatelets: Ion-Exchange Intercalation and Cell Imaging. *Chem. Commun.* **2013**, *49*, 9549−9551.
(22) Zhang, X.; Chi, Z.; Li, H.; Xu, B.; Li, X.; Liu, S.; Zhang, Y.; Xu, J. Synthesis and Properties of Novel Aggregation-Induced Emission Compounds with Combined Tetraphenylethylene and Dicarbazolyl Triphenylethylene Moieties. *J. Mater. Chem.* **2011**, *21*, 1788−1796.
(23) Yuan, Y.; Kwok, R. T. K.; Tang, B. Z.; Liu, B. Targeted Theranostic Platinum(IV) Prodrug with a Built-In Aggregation-Induced Emission Light-Up Apoptosis Sensor for Noninvasive Early Evaluation of Its Therapeutic Responses in Situ. *J. Am. Chem. Soc.* **2014**, *136*, 2546−2554.
(24) Zhang, X.; Zhang, X.; Tao, L.; Chi, Z.; Xu, J.; Wei, Y. Aggregation Induced Emission-Based Fluorescent Nanoparticles: Fabrication Methodologies and Biomedical Applications. *J. Mater. Chem. B* **2014**, *2*, 4398−4414.
(25) Zhang, Y.; Chen, Y.; Li, X.; Zhang, J.; Chen, J.; Xu, B.; Fu, X.; Tian, W. Folic Acid-Functionalized AIE Pdots Based on Amphiphilic PCL-*b*-PCL for Targeted Cell Imaging. *Polym. Chem.* **2014**, *5*, 3824−3830.
(26) Hu, R.; Ye, R.; Lam, J. W. Y.; Li, M.; Leung, C. W. T.; Tang, B. Conjugated Polyelectrolytes with Aggregation-Enhanced Emission Characteristics: Synthesis and Their Biological Applications. *Chem.—Asian J.* **2013**, *8*, 2436−2445.
(27) Zhang, X.; Zhang, X.; Yang, B.; Hui, J.; Liu, M.; Chi, Z.; Liu, S.; Xu, J.; Wei, Y. Facile Preparation and Cell Imaging Applications of Fluorescent Organic Nanoparticles That Combine AIE Dye and Ring-Opening Polymerization. *Polym. Chem.* **2014**, *5*, 318−322.
(28) Zhang, X.; Liu, M.; Yang, B.; Zhang, X.; Wei, Y. Tetraphenylethene-Based Aggregation-Induced Emission Fluorescent Organic Nanoparticles: Facile Preparation and Cell Imaging Application. *Colloids Surf., B: Biointerfaces* **2013**, *112*, 81−86.
(29) Sugihara, S.; Armes, S. P.; Blanazs, A.; Lewis, A. L. Non-Spherical Morphologies from Cross-Linked Biomimetic Diblock Copolymers Using RAFT Aqueous Dispersion Polymerization. *Soft Matter* **2011**, *7*, 10787−10793.
(30) Li, H.; Zhang, X.; Zhang, X.; Yang, B.; Yang, Y.; Wei, Y. Ultra-Stable Biocompatible Cross-Linked Fluorescent Polymeric Nanoparticles Using AIE Chain Transfer Agent. *Polym. Chem.* **2014**, *5*, 3758−3762.
(31) Li, H.; Zhang, X.; Zhang, X.; Yang, B.; Yang, Y.; Wei, Y. Stable Cross-linked Fluorescent Polymeric Nanoparticles for Cell Imaging. *Macromol. Rapid Commun.* **2014**, *35*, 1661−1667.
(32) Zhang, X.; Liu, M.; Yang, B.; Zhang, X.; Chi, Z.; Liu, S.; Xu, J.; Wei, Y. Cross-Linkable Aggregation Induced Emission Dye Based Red Fluorescent Organic Nanoparticles and Their Cell Imaging Applications. *Polym. Chem.* **2013**, *4*, 5060−5064.
(33) Yang, Z.; Yuan, Y.; Jiang, R.; Fu, N.; Lu, X.; Tian, C.; Hu, W.; Fan, Q.; Huang, W. Homogeneous Near-Infrared Emissive Polymeric Nanoparticles Based on Amphiphilic Diblock Copolymers with Perylene Diimide and PEG Pendants: Self-Assembly Behavior and Cellular Imaging Application. *Polym. Chem.* **2014**, *5*, 1372−1380.
(34) Bao, B.; Tao, N.; Yang, D.; Yuwen, L.; Weng, L.; Fan, Q.; Huang, W.; Wang, L. A Controllable Approach to Development of Multi-Spectral Conjugated Polymer Nanoparticles with Increased Emission for Cell Imaging. *Chem. Commun.* **2013**, *49*, 10623−10625.
(35) Wang, Z.; Chen, S.; Lam, J. W. Y.; Qin, W.; Kwok, R. T. K.; Xie, N.; Hu, Q.; Tang, B. Z. Long-Term Fluorescent Cellular Tracing by the Aggregates of AIE Bioconjugates. *J. Am. Chem. Soc.* **2013**, *135*, 8238−8245.
(36) Yang, C.-M.; Lai, Y.-W.; Kuo, S.-W.; Hong, J.-L. Complexation of Fluorescent Tetraphenylthiophene-Derived Ammonium Chloride to Poly (*N*-isopropylacrylamide) with Sulfonate Terminal: Aggregation-Induced Emission, Critical Micelle Concentration, and Lower Critical Solution Temperature. *Langmuir* **2012**, *28*, 15725−15735.


DOI: 10.1021/am5085308
*ACS Appl. Mater. Interfaces* 2015, 7, 4241−4246